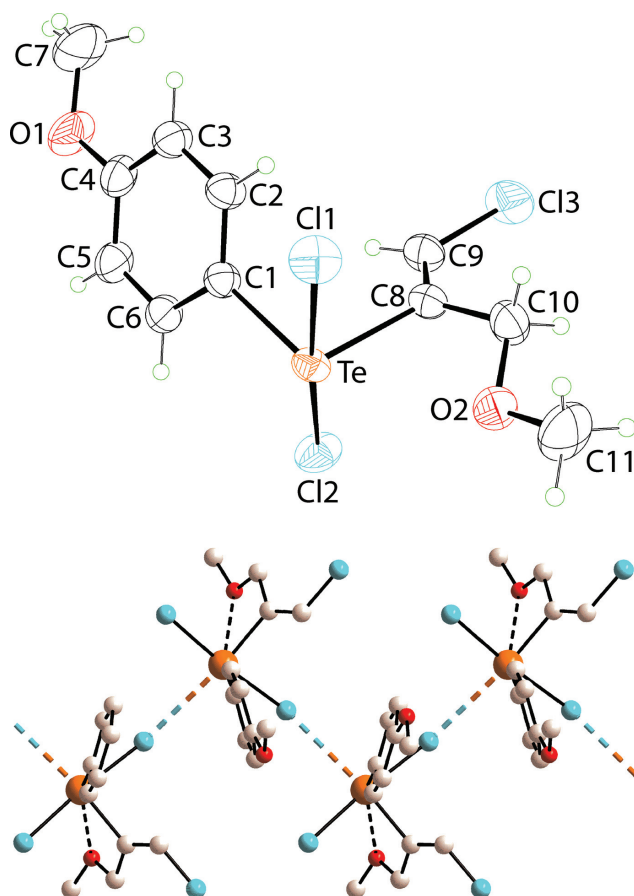




Ignez Caracelli*, Julio Zukerman-Schpector, Rodrigo L.O.R. Cunha and Edward R.T. Tiekink*

Crystal structure of (*E*)-dichloro(1-chloro-3-methoxyprop-1-en-2-yl)(4-methoxyphenyl)- λ^4 -tellane, $C_{11}H_{13}Cl_3O_2Te$



Abstract

$C_{11}H_{13}Cl_3O_2Te$, monoclinic, $P2_1/c$ (no. 14), $a = 11.0098(8)$ Å, $b = 16.471(1)$ Å, $c = 8.4975(7)$ Å, $\beta = 99.421(7)^\circ$, $V = 1520.17(19)$ Å³, $Z = 4$, $R_{gt}(F) = 0.0306$, $wR_{ref}(F^2) = 0.0852$, $T = 293(2)$ K.

CCDC no.: 2023890

Table 1 contains crystallographic data and Table 2 contains the list of the atoms including atomic coordinates and displacement parameters.

Table 1: Data collection and handling.

Crystal:	Colourless irregular
Size:	0.42 × 0.30 × 0.15 mm
Wavelength:	Mo $K\alpha$ radiation (0.71073 Å)
μ :	2.47 mm ⁻¹
Diffractometer, scan mode:	Enraf Nonius TurboCAD4, ω
θ_{max} , completeness:	29.0°, >99%
$N(hkl)_{measured}$, $N(hkl)_{unique}$, R_{int} :	4298, 4045, 0.032
Criterion for I_{obs} , $N(hkl)_{gt}$:	$I_{obs} > 2 \sigma(I_{obs})$, 3267
$N(param)_{refined}$:	157
Programs:	Absorption correction [1], Cad4 [2, 3], SIR2014 [4], SHELXL [5], WinGX/ORTEP [6]

Source of material

To a suspension of 4-methoxyphenyl tellurium trichloride in benzene, 3-methoxyprop-1-yne was added. The obtained 15:12:1 mixture of isomeric dichlorides was reduced with a saturated sodium thiosulfate solution leading to a mixture of tellurides prone to separation by column chromatography. After separation, the major isomer was converted to the title compound by treatment with sulfonyl chloride in dichloromethane and crystallised from a mixture of dichloromethane and hexanes leading to colourless crystals. Crystals of (I) were obtained from recrystallisation from its $CHCl_3$ solution. **M. Pt.:** 498–499 K. **Micronalysis:** Anal. C, 32.13; H, 3.19%. Calcd. for $C_{11}H_{13}Cl_3O_2Te$: C, 32.21; H, 3.18%. **¹H NMR** (500 MHz, $CDCl_3$, r.t.): δ 8.22 (d, $J = 9.1$ Hz, 2H), 7.09 (d, $J = 9.1$ Hz, 2H), 6.52 (s, 1H), 4.64 (s, 2H), 3.89 (s, 3H), 3.61 (s, 3H). **¹³C NMR** (125 MHz, $CDCl_3$, r.t.): δ 162.5, 146.2, 136.6,

<https://doi.org/10.1515/ncrs-2020-0380>

Received July 21, 2020; accepted August 18, 2020; available online September 18, 2020

*Corresponding authors: **Ignez Caracelli**, BioMat, Departamento de Física, Universidade Federal de São Carlos, C.P. 676, São Carlos, SP, 13565-905, Brazil, e-mail: ignez@df.ufscar.br; and **Edward R.T. Tiekink**, Research Centre for Crystalline Materials, School of Science and Technology, Sunway University, 47500 Bandar Sunway, Selangor Darul Ehsan, Malaysia, e-mail: edwardt@sunway.edu.my. <https://orcid.org/0000-0003-1401-1520>

Julio Zukerman-Schpector: Laboratório de Cristalografia, Estereodinâmica e Modelagem Molecular, Departamento de Química, Universidade Federal de São Carlos, C.P. 676, São Carlos, SP, 13565-905, Brazil

Rodrigo L.O.R. Cunha: Centro de Ciências Naturais e Humanas, Universidade Federal do ABC, 09210-170, Santo André, SP, Brazil

Table 2: Fractional atomic coordinates and isotropic or equivalent isotropic displacement parameters (Å²).

Atom	<i>x</i>	<i>y</i>	<i>z</i>	<i>U</i> _{iso} [*] / <i>U</i> _{eq}
Te	0.72293(2)	0.13655(2)	0.81137(2)	0.04507(9)
Cl1	0.80518(9)	0.04336(6)	1.03270(12)	0.0654(2)
Cl2	0.64189(9)	0.22175(7)	0.57003(14)	0.0725(3)
Cl3	0.84040(11)	−0.03913(8)	0.43545(13)	0.0793(3)
O1	1.2423(3)	0.2845(2)	0.7963(5)	0.0922(11)
O2	0.5494(2)	0.00773(18)	0.7294(4)	0.0700(7)
C1	0.9005(3)	0.18611(19)	0.8154(4)	0.0475(7)
C2	1.0035(3)	0.1381(2)	0.8543(4)	0.0528(7)
H2	0.994792	0.084156	0.882604	0.063*
C3	1.1196(3)	0.1695(2)	0.8518(4)	0.0565(8)
H3	1.188719	0.136878	0.879171	0.068*
C4	1.1325(4)	0.2490(2)	0.8089(5)	0.0635(9)
C5	1.0286(4)	0.2985(2)	0.7735(5)	0.0683(11)
H5	1.037507	0.352906	0.748237	0.082*
C6	0.9140(3)	0.2672(2)	0.7761(5)	0.0599(9)
H6	0.844881	0.300217	0.751527	0.072*
C7	1.3485(4)	0.2345(4)	0.8163(9)	0.115(2)
H7A	1.366135	0.215958	0.924781	0.173*
H7B	1.417260	0.265064	0.791731	0.173*
H7C	1.334114	0.188619	0.746083	0.173*
C8	0.7389(3)	0.0380(2)	0.6559(4)	0.0496(7)
C9	0.8207(3)	0.0396(2)	0.5607(4)	0.0566(8)
H9	0.870240	0.085374	0.560886	0.068*
C10	0.6491(4)	−0.0279(2)	0.6721(5)	0.0648(10)
H10A	0.621526	−0.053311	0.569472	0.078*
H10B	0.686976	−0.068992	0.745895	0.078*
C11	0.4712(5)	−0.0507(4)	0.7829(7)	0.0984(17)
H11A	0.443029	−0.088023	0.697977	0.148*
H11B	0.401829	−0.023894	0.814980	0.148*
H11C	0.515815	−0.079781	0.871921	0.148*

128.4, 119.2, 115.8, 68.0, 59.7, 55.5. ¹²⁵Te NMR (157.97 MHz, CDCl₃, r.t) δ 906.5.

Experimental details

The C-bound H atoms were geometrically placed (C–H = 0.93–0.97 Å) and refined as riding with *U*_{iso}(H) = 1.2–1.5*U*_{eq}(C). Owing to poor agreement, one reflection, i.e. (3 9 1), was omitted from the final cycles of refinement. A correction for extinction effects was applied with a final co-efficient = 0.0078(5).

Comment

While not as well recognised as selenium compounds, tellurium species are known to exhibit exciting biological responses [7, 8]. Experiments [9], confirmed by molecular docking studies [10], indicate that cysteine proteases, such as Cathepsin B, are key targets for thiophilic tellurium compounds, owing to the presence of a cysteine residue in the active site. This is important as the inhibition of Cathepsin

B results in the disruption of crucial cellular processes. It was in this connection that the title compound was originally synthesised among an extensive series of related derivatives [11]; experiments showed (I) not to be an effective inhibitor of Cathepsin B.

The molecular structure of (I) is illustrated in the upper part of the figure (35% displacement ellipsoids) and features a Te(IV) centre coordinated by *ipso*-C [Te–C1 = 2.114(3) Å], vinyl-C [Te–C8 = 2.118(3) Å] and two Cl–Te–Cl1 = 2.4811(9) Å and Te–Cl2 = 2.5243(10) Å atoms. The immediate coordination geometry about the tellurium(IV) centre is therefore, Ψ-trigonal bipyramid with the stereochemically active lone-pair of electrons occupying the third position in the equatorial plane. However, other close contacts are evident, such as an intramolecular Te···O(methoxy) interaction of 2.864(3) Å. Further, there is an intermolecular Te···Cl secondary bonding [12, 13] interaction with Te···Cl2ⁱ = 3.4229(12) Å for symmetry operation (i): *x*, 1/2 − *y*, 1/2 + *z*. The participation of the Cl2 atom in the secondary bonding interaction accounts for the elongation of the Te–Cl2 bond length compared with the Te–Cl1 bond. Taking into consideration the additional Te···O and Te···Cl interactions, the coordination geometry may therefore be described as Ψ-pentagonal-bipyramidal with the lone-pair of electrons occupying the fifth position in the equatorial plane. The result of the intermolecular Te···Cl interactions is the formation of a supramolecular chain with a zig-zag topology (glide symmetry) along the *c*-axis as shown in the lower part of the figure.

There are four direct literature precedents for (I), namely, the (4-MeOC₆H₄)Te[C(CMe₂OH)=C(H)Cl]Cl₂ [14], two conformational polymorphs of (4-MeOC₆H₄)Te{C(C(H)(OH)(CH₂)₅)=C(H)Ph}Cl₂ [15] and (4-MeOC₆H₄)Te[C(Ph)=C(H)SPh]Cl₂ [16], each of which features the same C₂TeCl₂ core as in (I), with a Ψ-trigonal-bipyramidal geometry, along with intramolecular Te···O or Te···S interactions.

In the crystal, the supramolecular chains are connected by methylene-C–H···O(methoxy) [C10–H10b···O1ⁱ: H10b···O1ⁱ = 2.58 Å, C10···O1ⁱ = 3.308(5) Å with angle at H10b = 132° for symmetry operation (ii) 2 − *x*, −1/2 + *y*, 3/2 − *z*] and methyl-C–H···Cl(Te-bound) [C11–H11b···Cl1ⁱⁱⁱ: H11b···Cl1ⁱⁱⁱ = 2.82 Å, C11···Cl1ⁱⁱⁱ = 3.646(6) Å with angle at H11b = 145° for (iii): 1 − *x*, −*y*, 2 − *z*] interactions to consolidate the three-dimensional packing.

Additional insight into the supramolecular association was accomplished by calculating the Hirshfeld surface as well as the full and decomposed two-dimensional fingerprint plots employing Crystal Explorer 17 [17] and standard protocols [18]. The most dominant contacts to the calculated surface are due to H···Cl/Cl···H contacts, at 37.7%, followed closely by H···H contacts, at 33.8%. Other prominent contacts arise from H···O/O···H [9.3%], H···C/C···H [6.3%]

and C···C [3.1%] contacts. The percentage contribution from Cl···Te/Te···Cl contacts is only 1.8% with Cl···Cl contacts contributing 1.7% but, at separations greater than the sum of the van der Waals radii.

Acknowledgements: The Brazilian agencies the Coordination for the Improvement of Higher Education Personnel, CAPES, Finance Code 001, the National Council for Scientific and Technological Development (CNPq) are acknowledged for grants (312210/2019–1, 433957/2018–2 and 406273/2015–4) to IC, (402289/2013-7 and 487012/2012-7) to RLOR and for a fellowship (303207/2017–5) to JZS. RLOR also acknowledges the Multi-User Central Facilities (CEM/UFABC) for experimental support and the Sustainable Technologies Unit of UFABC (NuTS). Sunway University Sdn Bhd is thanked for financial support of this work through Grant No. STR-RCTR-RCCM-001–2019.

References

1. North, A. C. T.; Phillips, D. C.; Mathews, F. S.: A semi-empirical method of absorption correction. *Acta Crystallogr.* **A24** (1968) 351–359.
2. CAD4 Express Software. Enraf-Nonius, Delft, The Netherlands (1994).
3. Harms, K.; Wocadlo, S.: XCAD4 – CAD4 Data Reduction. Program for Processing CAD-4 Diffractometer Data. University of Marburg, Germany (1995).
4. Burla, M. C.; Caliendo, R.; Carrozzini, B.; Cascarano, G. L.; Cuocci, C.; Giacovazzo, C.; Mallamo, M.; Mazzone, A.; Polidori, G.: Crystal structure determination and refinement via SIR2014. *J. Appl. Cryst.* **48** (2015) 306–309.
5. Sheldrick, G. M.: Crystal structure refinement with SHELXL. *Acta Crystallogr.* **C71** (2015) 3–8.
6. Farrugia, L. J.: WinGX and ORTEP for Windows: an update. *J. Appl. Cryst.* **45** (2012) 849–854.
7. Tiekink, E. R. T.: Therapeutic potential of selenium and tellurium compounds: opportunities yet unrealised. *Dalton Trans.* **41** (2012) 6390–6395.
8. Seng, H.-L.; Tiekink, E. R. T.: Anti-cancer potential of selenium- and tellurium-containing species: opportunities abound! *Appl. Organomet. Chem.* **26** (2012) 655–662.
9. Silberman, A.; Kalechman, Y.; Hirsch, S.; Erlich, Z.; Sredni, B.; Albeck, M.: The anticancer activity of organotelluranes: potential role in integrin inactivation. *ChemBioChem* **17** (2016) 918–927.
10. Caracelli, I.; Maganhi, S. H.; de Oliveira Cardoso, J.; Cunha, R. L. O. R.; Vega-Tejido, M. A.; Zukerman-Schpector, J.; Tiekink, E. R. T.: Crystallographic and docking (Cathepsins B, K, L and S) studies on bioactive halotelluroxetanes. *Z. Kristallogr. Cryst. Mater.* **233** (2018) 113–124.
11. Cunha, R. L. O. R.; Gouvêa, I. E.; Feitosa, G. P. V.; Alves, M. F. M.; Brömme, D.; Comasseto, J. V.; Tersariol, I. L. S.; Juliano, L.: Irreversible inhibition of human cathepsins B, L, S and K by hypervalent tellurium compounds. *Biol. Chem.* **390** (2009) 1205–1212.
12. Alcock, N. W.: Secondary bonding to nonmetallic elements. *Adv. Inorg. Chem. Radiochem.* **15** (1972) 1–58.
13. Tiekink, E. R. T.: Supramolecular assembly based on “emerging” intermolecular interactions of particular interest to coordination chemists. *Coord. Chem. Rev.* **345** (2017) 209–228.
14. Zukerman-Schpector, J.; Camillo, R. L.; Comasseto, J. V.; Cunha, R. L. O. R.; Chieffi, A.; Zeni, G.; Caracelli, I.: Dichloro [(E)-2-chloro-1-(2-hydroxyprop-2-yl)vinyl](4-methoxyphenyl)-tellurium(IV). *Acta Crystallogr.* **C55** (1999) 1339–1342.
15. Tejjido, M. V.; Zukerman-Schpector, J.; Camillo, R. L.; Caracelli, I.; Stefani, H. A.; Chieffi, A.; Comasseto, J. V.: Dichloro [(E)-2-chloro-1-vinyl-cyclohexanol](4-methoxy phenyl)Te(IV). a case of conformational polymorphism. *Z. Kristallogr. Cryst. Mater.* **218** (2003) 636–641.
16. Zukerman-Schpector, J.; Caracelli, I.; Dabdoub, M. J.; Dabdoub, V. B.; Pereira, M. A.: (Z)-1-(Dichloro-*p*-methoxyphenyltelluro)-1-phenyl-2-thiophenylethene. *Acta Crystallogr.* **C52** (1996) 2772–2774.
17. Turner, M. J.; McKinnon, J. J.; Wolff, S. K.; Grimwood, D. J.; Spackman, P. R.; Jayatilaka, D.; Spackman, M. A.: Crystal Explorer v17. The University of Western Australia, Australia (2017).
18. Tan, S. L.; Jotani, M. M.; Tiekink, E. R. T.: Utilizing Hirshfeld surface calculations, non-covalent interaction (NCI) plots and the calculation of interaction energies in the analysis of molecular packing. *Acta Crystallogr.* **E75** (2019) 308–318.